Molecular & Biochemical Parasitology 175 (2011) 58–67

Contents lists available at ScienceDirect

Molecular & Biochemical Parasitology

Phenylalanine hydroxylase (PAH) from the lower eukaryote *Leishmania major*☆

Lon-Fye Lye[a], Song Ok Kang[a], Joshua D. Nosanchuk[b], Arturo Casadevall[b], Stephen M. Beverley[a,*]

[a] *Department of Molecular Microbiology, Box 8230, Washington University Medicine School, 600 S. Euclid Ave., St. Louis, MO 63110, USA*
[b] *Department of Medicine, Albert Einstein College of Medicine, 1300 Morris Park Avenue, Bronx, New York, NY 10461, USA*

ARTICLE INFO

Article history:
Received 11 July 2010
Received in revised form
10 September 2010
Accepted 19 September 2010
Available online 29 September 2010

Keywords:
Trypanosomatid protozoa
Tetrahydrobiopterin
Aromatic amino acid hydroxylase
Amino acid metabolism
Virulence

ABSTRACT

Aromatic amino acid hydroxylases (AAAH) typically use tetrahydrobiopterin (H_4B) as the cofactor. The protozoan parasite *Leishmania major* requires biopterin for growth and expresses strong salvage and regeneration systems to maintain H_4B levels. Here we explored the consequences of genetic manipulation of the sole *L. major* phenylalanine hydroxylase (*PAH*) to explore whether it could account for the *Leishmania* H_4B requirement. *L. major PAH* resembles AAAHs of other organisms, bearing eukaryotic-type domain organization, and conservation of key catalytic residues including those implicated in pteridine binding. A *pah*$^-$ null mutant and an episomal complemented overexpressing derivative (*pah*−/+*PAH*) were readily obtained, and metabolic labeling studies established that *PAH* was required to hydroxylate Phe to Tyr. Neither WT nor overexpressing lines were able to hydroxylate radiolabeled tyrosine or tryptophan, nor to synthesize catecholamines. WT but not *pah*$^-$ parasites showed reactivity with an antibody to melanin when grown with L-3,4-dihydroxyphenylalanine (L-DOPA), although the reactive product is unlikely to be melanin *sensu strictu*. WT was auxotrophic for Phe, Trp and Tyr, suggesting that PAH activity was insufficient to meet normal Tyr requirements. However, *pah*$^-$ showed an increased sensitivity to Tyr deprivation, while the *pah*$^-$/+*PAH* overexpressor showed increased survival and could be adapted to grow well without added Tyr. *pah*$^-$ showed no alterations in H_4B-dependent differentiation, as established by *in vitro* metacyclogenesis, or survival in mouse or macrophage infections. Thus *Leishmania PAH* may mitigate but not alleviate Tyr auxotrophy, but plays no essential role in the steps of the parasite infectious cycle. These findings suggest *PAH* is unlikely to explain the *Leishmania* requirement for biopterin.

1. Introduction

Leishmania is a genus of trypanosomatid protozoan parasites comprising more than 20 species responsible for a number of severe diseases of humans worldwide, infecting over 12 million people [1]. *Leishmania* are transmitted by the bite of Phlebotomine sand flies, and in the mammalian host reside primarily in an acidified phagolysosome of macrophages, where they must deflect host defenses and immune responses in order to survive [2]. As a deep-branching eukaryotic lineage, *Leishmania* exhibits considerable divergence in its metabolic enzyme repertoire [3], providing opportunities for basic studies as well as more practical efforts towards improved chemotherapy.

Here we focus on genetic studies of null and overexpression mutants of the sole *Leishmania* gene related to aromatic amino acid hydroxylases (AAAH). Our interest in AAAHs arose because their cofactor biopterin is an essential growth factor, distinct from folate, for several trypanosomatid species. In mammals tetrahydrobiopterin (H_4B) is required by several enzymes of critical metabolic importance, including amino acid hydroxylases (AAAHs), nitric oxide synthase and the ether lipid cleavage monooxygenase (reviewed in [4,5]). *Leishmania* and other trypanosomatids are general auxotrophs for pteridines [6,7], and acquire biopterin from the host by salvage, first by uptake by the transporter BT1 [8,9] and then reduction to H_4B by the broad spectrum pteridine reductase PTR1 ([10], reviewed by [11,12]). The direct pteridine product of AAAH action is 4α-OH-H_4B (carbinolamine) which is returned to H_4B through the successive action of pteridine-4-carbinolamine dehydratase (PCD) and *quininoid* dihydropteridine reductase [QDPR; 4]. Trypanosomatids encode functional forms of both genes [13,14].

Despite knowledge of H_4B metabolism and requirements in *Leishmania*, the essential metabolic role of H_4B is not established [15]. In other species, AAAH activity requires the

Abbreviations: PAH, phenylalanine hydroxylase; AAAH, aromatic amino acid hydroxylase; *LmjPAH*/LmPAH, *Leishmania major* phenylalanine hydroxylase gene/enzyme; H_2B, dihydrobiopterin; H_4B, tetrahydrobiopterin; bp, base pair(s); ORF, open reading frame; nt, nucleotide(s); PCR, polymerase chain reaction; Phe, phenylalanine; Tyr, tyrosine; Trp, tryptophan; WT, wild-type; L-DOPA, L-dihydroxyphenylalanine.

☆ The nucleotide sequences reported in this paper have been submitted to the GenBank™/EBI Data bank with accession number AY273788.

* Corresponding author. Tel.: +1 314 747 2630; fax: +1 314 747 2634.
E-mail address: beverley@borcim.wustl.edu (S.M. Beverley).

0166-6851/$ – see front matter © 2010 Elsevier B.V. All rights reserved.
doi:10.1016/j.molbiopara.2010.09.004

amino acid substrate, molecular oxygen, and the reduced cofactor H_4B ((6R)-L-erythro-5,6,7,8-tetrahydropterin; [16]). AAAHs catalyze the conversion of phenylalanine, tyrosine and/or tryptophan to tyrosine, 3,4-dihydroxyphenylalanine (L-DOPA), or 5-hydroxytryptophan, respectively. Typically these activities are carried out by different enzymes, phenylalanine hydroxylase (PAH; EC 1.14.16.1), tyrosine hydroxylase (TyrH; EC 1.14.16.2) and tryptophan hydroxylase (TrpH; EC 1.14.16.4), although in some organisms these hydroxylases can show broader specificities (reviewed in [16,17]). AAAHs are widespread in evolution, being found in prokaryotes, protozoans, plants, fungi, and animals. In metazoans AAAHs play critical roles in metabolism and neurotransmitter synthesis, and PAH participates in Phe catabolism in bacteria [18].

The identification of a putative H_4B-dependent AAAH in the *Leishmania* genome raised the possibility that this activity might account for its H_4B biopterin requirement. We report here studies that confirm the activity of Phe hydroxylase (PAH) in *L. major*, and characterize its role in parasite metabolism and infectivity.

2. Materials and methods

2.1. Chemicals and reagents

Dihydrobiopterin (H_2B) was from Schircks Laboratories (Jona, Switzerland). Biopterin, epinephrine, norepinephrine, propanolol and RPMI 1640 vitamin solutions were from Sigma–Aldrich (St. Louis, USA). L-[5-^{3}H] tryptophan, L-[3,5-^{3}H] tyrosine, and L-[2,6-^{3}H] phenylalanine) were obtained from Amersham Biosciences Corp. Phenol red solution and penicillin/streptomycin was from Invitrogen. Fetal calf serum was purchased from Bio-Whittaker and bovine serum albumin (Fraction V) from U.S. Biochemical Corp. M199 with Hanks's salts was from US Biologicals. Folate-deficient medium (fdM199) was custom manufactured by Invitrogen and is identical to M199 except lacking folate and thymidine [19].

2.2. Parasite and growth media

L. major Friedlin V1 (MHOM/JL/80/Friedlin) recovered from infected animals were used within 10 serial passages *in vitro*. Promastigotes were grown in M199 medium supplemented with 10% heat-inactivated fetal bovine serum at 26 °C [19]; for routine culture 2 μg ml^{-1} biopterin was added. Metacyclic promastigotes were purified from a stationary phase cells using the negative agglutination assay [20]. Amastigotes were harvested from BALB/c mice footpad lesion 3 weeks postinfection.

In some experiments cells were grown in fdM199 (M199 medium lacking folate and thymidine supplemented with 0.66% bovine serum albumin rather than serum). To deplete internal levels of biopterin, WT and KO cells were grown in fdM199 medium lacking biopterin for three passages (dilution of cells to ~2×10^5/ml and growth into stationary phase at about 2×10^7/ml). For differentiation, biopterin-depleted cells were incubated at a cell density of 2×10^5 cells/ml in fdM199 medium supplemented with biopterin (0.001 μg ml^{-1} or 2 μg ml^{-1}), or without biopterin plus 100 μM epinephrine, 100 μM norepinephrine or 10 μM propanolol. Alternatively, an RPMI 1640 based medium was used, containing 1% fetal bovine serum, 40 mM Hepes pH 7.4, 1× RPMI 1640 vitamin mix, 1× amino acid mixtures (lacking Phe, Tyr or Trp), 100 μM adenine, 1 μg ml^{-1} biotin, 5 μg ml^{-1} hemin, 50 U ml^{-1} penicillin, 50 μg ml^{-1} streptomycin, 2 μg ml^{-1} biopterin, 5.37 mM KCl, 0.42 mM $Ca(NO_3)_2 \cdot 4H_2O$, 102.67 mM NaCl, 5.63 mM Na_2HPO_4, 0.41 mM $MgSO_4 \cdot 7H_2O$, 23.81 mM $NaHCO_3$, 11.11 mM glucose, and 0.0005% phenol red. Complete media additionally contained Phe (91 μM), Tyr (111 μM) and Trp (24 μM).

2.3. Southern and Northern blot analysis

L. major FV1 genomic DNA was isolated from the late logarithmic phase promastigotes by the LiCl method [22]. Genomic DNA was digested with the appropriate restriction enzymes and electrophoreses on 0.8% agarose gels and transferred to nylon membranes. Total RNA of *L. major* promastigotes and amastigotes was isolated using the phenol/guanidine isothiocyanate reagent TRIzol™ (Invitrogen) according to the manufacturer's instructions. Southern and Northern were performed following standard procedures and the hybridization probes were labeled with a [α-^{32}P] dCTP by random-priming [23].

2.4. PAH gene cloning and sequencing

A fragment spanning 870 nt to 953 nt of the *PAH* ORF) was obtained by PCR amplification (primers SMB1076 5′-GCCGGAC ATGGTTCACGACATC and SMB1077 5′-AGGCCGATCGTCTGGGTG AAG) and GSS clone lm94b04 [24] DNA template. This DNA was radiolabeled and used to screen an *L. major* Friedlin V1 cosmid library [25]. Three different cosmid clones containing *PAH* gene were obtained (c11p6, strain B4089; c10m17, strain B4086; c9o9, strain B4087). Following subcloning and mapping, the sequence of the *PAH* was determined using the ABI PRISM™ BigDye Terminator Cycle Sequencing Ready Reaction kit (PE Applied Biosystems, Foster City, CA).

2.5. Mapping the 5′ terminus of the mature PAH transcript

To amplify the 5′-end of *PAH*, *L. major* total RNA was used as a template for RT-PCR. Reverse transcription was performed with Superscript II reverse transcriptase (Invitrogen) following the manufacturer's protocol. PCR was performed using Taq polymerase (Roche) with 30 cycles of denaturing at 94 °C for 1 min, annealing at 50 °C for 1 min and extension at 72 °C for 2 min. Primers specific for the *L. major* spliced leader sequence (SMB936: 5′-ACCGCTATATAAG TATCAGTTCTGTACTTTA) and two specific primers, SMB1122 and 1117 located within the *PAH* coding region (SMB1122: 5′-TGCAGG GACGTGCGGCACCGCG and SMB1117: 5′-GTCGGGTACAGGCG GGTCAGGT). The PCR products were purified and sequenced directly.

2.6. Overexpression of PAH

The 1362-nt *PAH* open reading frame was amplified by PCR with Pfu polymerase (Stratagene) using primers SMB 1155 (5′-GCGGAT**CCACC**ATGCTGCTGCGCAGTCGTTTGT; the underline sequence corresponds to a *BamH*I site and the bold nucleotides correspond to a "Kozak" sequence), SMB 1156 (5′-CGGGATCCTTAGAAGGTGAAGTTTGTTCGC), and 50 ng of template genomic DNA. The amplified DNA fragment was digested and cloned into the *BamH*I site of the *Leishmania* expression vector pXG1a [26], yielding pXG-PAH (strain B4193), whose sequence was confirmed.

2.7. Molecular constructs for replacement of PAH alleles and transfection

The 5′-flanking region of the *PAH* gene was amplified by PCR using the primers SMB1589 (5′-CGGGGTACCGACGACAGACGTG CCG) and SMB1590 (5′-CCATCGATCTTATTCTCGAGGCAAGTCAGG) adding *Kpn*I/*Cla*I sites, while the 3′ flanking region was PCR amplified using primers SMB1608 and 1592 adding *BamH*I/*Not*I sites. These fragments were digested with the appropriate enzymes and inserted successively into pBSKII (Promega, Madison, WI), yielding (pBS5′3′PAH). Then, *BSD* and *HYG* resistance

ORFs were amplified individually with primers SMB1666 (5′-CCCAAGCTTATGGCCAAGCCTTTGTCTCAAGA)/SMB1667 (5′-CGGGATCCTTAGCCCTCCCACACATAACCAG) or SMB1665 (5′-CCCAAGCTTATGAAAAAGCCTGAACTCACCGC)/SMB1594 (5′-CGGGATCCCTATTCCTTTGCCCTCGGACGA), respectively, which added *Hind*III and *BamH*I sites, and templates pXG-HYG [27] and pXG-BSD [28]. These fragments were digested appropriately and inserted into *Hind*III/*BamH*I digested pBS5′3′PAH, yielding the final replacement constructs pBS5′BSD3′PAH and pBS5′HYG3′PAH (strain B4696, strain B4692). DNAs were cut with *Not*I and *Kpn*I, and the targeting fragment purified. WT parasites were electroporated with the *PAH::HYG* targeting fragment derived from B4692 as described [21]. Transfectant colonies were obtained after plating on semisolid M199 medium containing hygromycin B (50 μg ml^{-1}), with typical frequencies. Three bearing heterozygous replacements (formally *PAH*/*PAH::ΔHYG*) were passaged through animals where they showed typical infectivity. One (clone 2) was selected and electroporated with the *PAH::BSD* targeting fragment, and, and transfectant colonies obtained after plating on semisolid M199 medium containing blasticidin (10 μg ml^{-1}) and hygromycin B (50 μg ml^{-1}), again at normal frequencies. Following molecular confirmation several lines (formally *PAH::ΔHYG*/*PAH::ΔBSD*, referred to as *pah*$^{-}$ hereafter) where used to infect animals where they showed typical infectivity, as described elsewhere in the text. One of these (KO4) was selected and electroporated with pXG-PAH, and transfectant colonies obtained following plating on semisolid media containing G418 (10 μg ml^{-1}), blasticidin (10 μg ml^{-1}) and hygromycin B (50 μg ml^{-1}). Several lines (formally, *PAH::ΔHYG*/*PAH::ΔBSD* [pXG-PAH], referred to as *pah*$^{-}$/+*PAH* hereafter) were passaged through animals where they showed typical infectivity, and one (KO4-AB2) was selected.

2.8. Metabolic labeling

Leishmania major were grown in M199 medium until early log phase (2×10^6/ml), harvested by centrifugation, and washed twice and incubated further in modified RPMI 1640 medium whose aromatic amino acid contents was adjusted as follows. For Phe labeling, media contained 23 μM Phe and 8 μM Trp, while for Tyr and Trp labeling 23 μM Phe, 28 μM Tyr and 28 μM Trp were used. Cells were resuspended in 1 ml of medium at final concentration of 5×10^7/ml, and 10 μl of a 1 mCi/ml stock of radiolabeled L-(2,6-^{3}H) phenylalanine, L-(3,5-^{3}H) tyrosine or L-(5-^{3}H) trytophan added (Phe, 480 Ci/mmol, Tyr 55 Ci/mmol or Trp, 32 Ci/mmol). Cells were incubated for 2 h at 26 °C, and then placed over 200 μl of dibutylphthalate and centrifuged 14,000 × *g* for 2 min. The upper aqueous layer was removed, and residual surface material was removed by washing twice with 1 ml of PBS. The oil layer was then removed, and the cells were recovered and resuspended in 100 μl of PBS.

For total amino acid uptake, 50 μl of suspended cells was lysed with 200 μl of 1% Triton X-100, added to 5 ml of Scintiverse II scintillation fluid, and used for liquid scintillation counting. For HPLC analysis, 50 μl of cell suspension was heated at 100 °C for 10 min, and centrifuged at 14,000 × *g* for 15 min. Then, samples were derivatized as described [29] with some modifications. Briefly, 10–50 μl of cell lysate was mixed with 110 μl of borate buffer (0.2 M sodium borate, 1 mM EDTA, pH 8.8) and mixed by vortexing. Then 40 μl of AccQ-Fluor reagent (*N*-hydroxysuccinimidyl-6-aminoquinoyl carbamate Waters, USA) was then added to give a final volume of 200 μl, the sample was vortexed vigorously, and 50 μl of derivatized sample was used for chromatography.

2.9. High performance liquid chromatography (HPLC)

A Waters HPLC and Millennium software was used for system control, data collection, and peak area calculation. HPLC columns and buffers were used as described [29], except Waters 600E gradient curve shape 7 was used instead of a linear gradient in order to improve separation of norepinephrine from valine. Unlabeled amino acids were included as standards as indicated. Fractions were collected at 1 min intervals, and 5 ml of Scintiverse II scintillation fluid was added prior to liquid scintillation counting.

2.10. Immunofluorescence

Ten microliter suspensions containing 10^6 *Leishmania* cells grown with or without L-DOPA were dried on poly-L-lysine-coated slides. The slides were washed in PBS, incubated in Superblock® [Pierce, Rockford, IL] blocking buffer for 1 h at 37 °C followed by incubation with 10 μg ml^{-1} of the melanin-binding monoclonal antibody 6D2 [30] for 1 h at 37 °C. After washing, the slides were incubated with a 1:1000 dilution of tetramethyl rhodamine isothiocyanate (TRITC)-conjugated goat anti-mouse IgM (Southern Biotechnologies Associates, Inc.; Birmingham, AL) for 1 h at 37 °C. Slides were washed, mounted using a 50% glycerol, 50% PBS, and 0.1 M *N*-propyl gallate solution, and viewed with an Olympus AX70 microscope (Melville, NY) equipped with a TRITC filter. Negative controls were incubated with mAb 5C11, which binds mycobacterial lipoarabinomannan [31] as the primary Ab, or TRITC-labeled Ab alone.

2.11. Melanin isolation

Promastigotes were suspended in 1.0 M sorbitol–0.1 M sodium citrate, pH 5.5. Cell wall lysing enzymes (from *Trichoderma harzianum*; Sigma–Aldrich, St. Louis) were added (10 mg ml^{-1}) and suspensions were incubated at 30 °C overnight. Cells were collected by centrifugation, washed with PBS, and incubated with 4 M guanidine thiocyanate 12 h. The particulate was treated with 1 mg ml^{-1} proteinase K (10 mM Tris, 1.0 mM $CaCl_2$, and 0.5% SDS, pH 7.8) at 37 °C overnight and then extracted three times with chloroform. The debris was collected, washed with PBS, and boiled in 6.0 M HCl for 1 h.

2.12. Mouse infectivity tests

BALB/c mice were from Charles River Laboratories Inc. (Wilmington, MA) and CBA/J mice from the Jackson Laboratory (Bar Harbor, Me). All studies were performed using protocols approved by the institutional animal studies committee. Parasites were grown to stationary phase in M199 medium, and groups of BALB/c mice were injected subcutaneously (s.c.) into the footpads with 10^6, 10^5, 10^4 parasites per mice [32]. Lesions were monitored by measuring the thickness of the footpad with a Vernier caliper. Lesion parasites were enumerated in the infected tissue by a limiting dilution assay [33].

2.13. Macrophage Infections

Infection of peritoneal macrophages with C3-opsonized parasites with performed as described [34]. The medium was changed daily, and at days 1, 2, 3 postinfection, intracellular parasites were visualized in formaldehyde-fixed macrophages by nuclear staining with Hoechst 33342 (0.5 μg ml^{-1}).

3. Results

3.1. Identification and properties of an L. major PAH gene

We identified a candidate phenylalanine hydroxylase gene in blast searches of data obtained from a whole genome shotgun library [24]. A radiolabeled probe was used to screen an *L.*

Fig. 1. Alignment of *L. major* PAH with human phenylalanine, tyrosine and tryptophan hydroxylases. The predicted amino acid sequence of *L. major* PAH (Lmaj) was aligned with human phenylalanine, tryptophan and tyrosine hydroxylase (HsPheH, TyrH and TrpH; accession numbers are provided in the legend to Fig. S3). Residues identical in two or more sequences are highlighted in gray boxes. Residues implicated in iron binding are marked by a '●', residues implicated in substrate or cofactor binding by a '▼', and residues associated with amino acid specificity by a '◊'. The presumptive N terminal 'regulatory' and C-terminal 'oligomerization' domains are marked by a solid box, while the region homologous to the pteridine binding region of other AAAH is marked by a dashed box.

major cosmid library, and the relevant regions of several cosmids were sequenced. The gene encoded a predicted protein of 453 aa/50.4 kDa (Fig. 1) and was given the gene symbol *PAH*, as it was subsequently shown below to be required for PAH activity. Southern blot analysis showed it to be present in a single copy (Fig. S1), in good agreement with the current *L. major* genome assembly, where *PAH* bears the systematic gene identifier LmjF28.1280 [35].

L. major PAH displayed an overall 42–51% identity to AAAH from mammals, *Drosophila* or *C. elegans*. Mammalian AAAHs contain a variable N terminal domain comprising about 1/3 of the protein that mediates regulatory functions, a central conserved catalytic domain, and a short C-terminal domain mediating oligomerization (reviewed in [16,17]). Similarly, LmjPAH showed a divergent N terminal domain comprising amino acids 1–123, a more conserved catalytic domain comprising amino acids 124–436, followed by a divergent C-terminal domain (Fig. 1). Recently two *PAH*s were described in *Toxoplasma gondii*, whose predicted proteins bearing signal sequences potentially indicative of secretion [36]. However, *L. major* PAH lacks an N-terminal extension (Fig. 1) and several computational methods did not predict a signal sequence for the *Leishmania* PAH.

Structural motifs characteristic of aromatic amino acid hydroxylases were found in the central catalytic region of LmjPAH, including the iron binding site (His295, His301, and Glu331 in LmjPAH) [37], and conserved substrate and cofactor binding sites (residues 274–301) [38]. LmjPAH contains Asp at the position corresponding to Glu286 of rat PheH, which has been implicated in H_4B binding [39]. While amino acid hydroxylases often show cross-activity to varying extents, and several studies have shown it is difficult to reliably predict amino acid specificity from amino acid sequences alone, some trends have been observed [16]. Several amino acid residues determined the substrate specific activity for tyrosine or tryptophan hydroxylase were not found in LmPAH. These include the position corresponding to Y235 and F313 in tryptophan hydroxylase [40] and D455 of tyrosine hydroxylase [41].

3.2. Structure and expression of PAH mRNA during the infectious cycle

In *Leishmania* and related trypanosomatid protozoans, every mRNA contains a 39-nt 'spliced-leader' at its 5′ end added by trans-splicing [42]. We used RT-PCR with a spliced-leader and two primers specific for PAH to map the 5′ trans-splice acceptor site of the PAH mRNA to an AG dinucleotide 141 nt 5′ of the predicted AUG initiation codon, which was also the first AUG (data not shown). Northern blots revealed a single 4 kb transcript in all stages of the infectious cycle (early log promastigote, late log promastigote, metacyclic promastigote and amastigote) with little variation during development (Fig. 2). A similar result was obtained with the mRNA encoding the H_4B regenerating enzyme QDPR [13].

3.3. Generation of PAH null mutants by targeted gene deletion

We were unable to express PAH in an enzymatically active form in *E. coli*, or in an active form *in vitro*, despite many attempts. These included varying expression conditions or host cells, tests of alternative pteridines including folates, or tests of truncations removing the poorly conserved N terminal 'regulatory' domain, or this as well as the C-terminal domain; several such variations had proven successful in studies of other species' AAAH. Thus we turned to studies of PAH null mutants, or parasites over-expressing PAH, to explore its potential roles and activities *in vivo*.

As *Leishmania* species are predominantly diploid, two successive rounds of gene targeting were required to generate null mutants [27]. The first *PAH* allele was replaced by the hygromycin B resistance marker (*HYG*) and the second was replaced with the blasticidin (*BSD*) resistance marker (Fig. 3A). Southern blot analysis

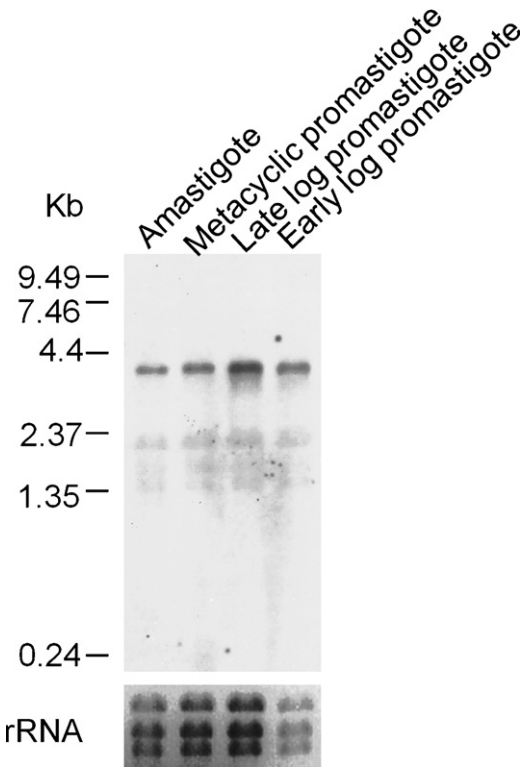

Fig. 2. Expression of *PAH* mRNA during the *Leishmania major* infectious cycle. Northern blot analysis of total RNAs probed with the *LmPAH* coding region sequence are shown. The autoradiogram is shown in the upper panel with the single ~4-kb *LmPAH* transcript. Molecular size markers (kb) are shown to the left. The lower panel shows the ethidium bromide-stained gel showing the three rRNAs as a loading control.

with a *PAH* probe confirmed that the PAH gene had been completely deleted (Fig. 3C), while hybridization with a flanking probe confirmed the replacements had occurred as planned (Fig. 3D). Notably, homozygous replacement (*pah*$^-$) lines were obtained a typical frequencies, and grew normally in standard M199 culture media thereafter. Several independent lines were analyzed, all of which had similar growth properties (not shown). We restored PAH expression by transfection of an episomal multicopy vector, yielding lines termed *pah*$^-$/+*PAH*, which additionally exhibit PAH overexpression.

3.4. In vivo detection of PAH-dependent phenylalanine hydroxylase activity by metabolic labeling

Leishmania were grown to logarithmic phase, collected, washed twice, and inoculated into media containing radiolabeled phenylalanine, tyrosine or tryptophan. After 2 h, samples were collected, deproteinized, and separated by HPLC after addition of the appropriate standards (Fig. 4A–C). When labeled with [^{3}H]-Phe, WT but not *pah*$^-$ extracts showed incorporation into a peak comigrating with the free Tyr standard (Fig. 4A). In contrast, no incorporation above background was seen using [^{3}H]-Tyr or [^{3}H]-Trp, into their predicted products DOPA or 5-hydroxy-tryptophan (Fig. 4B and C). Since limiting concentrations of radiolabeled essential amino acids were used in order to maximize the specific activity, and free amino acids are used in protein synthesis, in preliminary experiments we varied the time of labeling from 1 to 4 h. As before no further metabolism of radiolabeled Tyr or Trp was detected, while [^{3}H]-Tyr formation from [^{3}H]-Phe was maximal at 2 h. Other than Tyr formation, no differential was seen between WT and *pah*$^-$, or between the *pah*$^-$/+*PAH* overexpressor (data not shown). These data indicate that the *Leishmania* PAH is required for phenylalanine but not tyrosine or tryptophan hydroxylase activ-

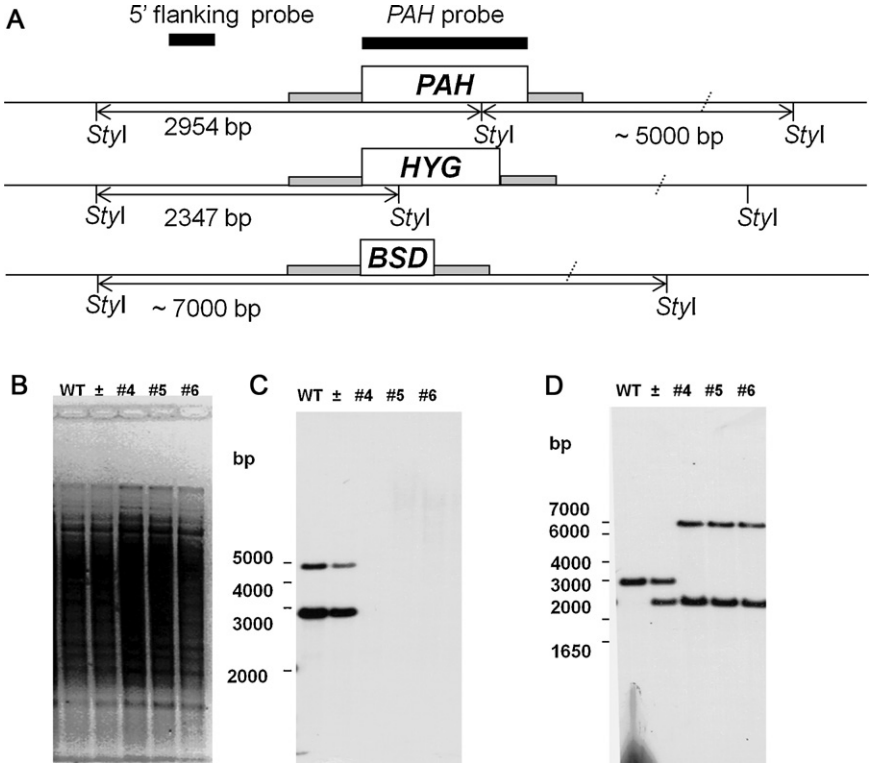

Fig. 3. Generation of *L. major PAH* null mutants. (A) Restriction map of the native *PAH* locus and planned *HYG* and *BSD* replacements. The position of *Sty*I sites and predicted fragment sizes are shown. Hybridization probes are shown by black bars, codon regions by open boxes, and regions contained within the targeting fragment by gray bars. (B–D) Southern blot analysis of wild type (WT), heterozygous (±) and *PAH null* mutant lines (#4, 5, and 6). DNA was subjected to Southern blot analysis using the radiolabeled *PAH* ORF (panel C) or a 5′ flanking (panel D) probes shown in panel A. Panel B shows the ethidium bromide stained gel prior to transfer.

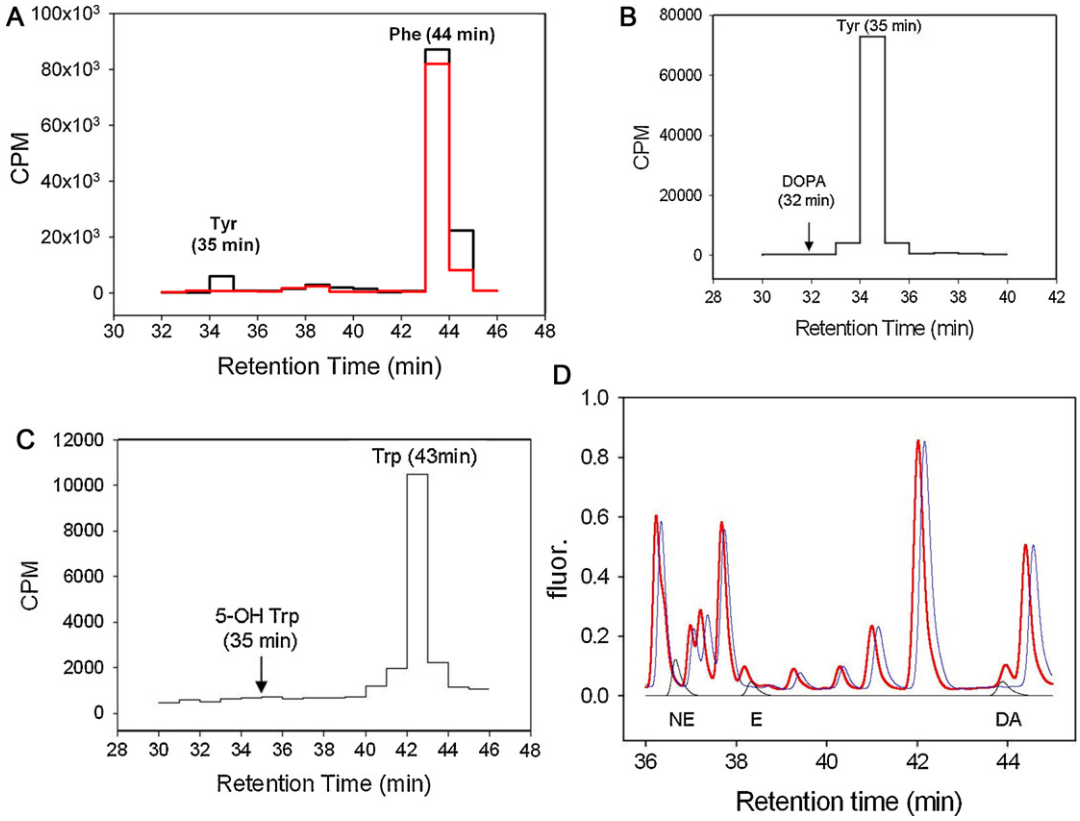

Fig. 4. Metabolic labeling with aromatic amino acids and catecholamine analysis of *L. major*. Panels A–C, WT (black lines) or *pah*⁻ (red line) were grown in the presence of [^{3}H] amino acids, and incorporation into free Phe, Tyr or Trp in deproteinized cell lysates was determined by liquid scintillation counting following derivatization and HPLC separation. Panel D, Analysis of *L. major* for the presence of catecholamines. Deproteinized lysates were separated by HPLC following derivatization as described in Section 2. The fluorescence traces are shown for WT (blue) and WT mixed with norepinephrine (NE), ephinephrine (E) and dopamine (DA) standards (red). Offset below these are traces (black) for separation of NE, E, and DA run individually.

ity. Potentially, PAH possess a low level of tyrosine hydroxylase activity not evident in our studies above. Thus we sought but were unable to detect by HPLC potential downstream catecholamine metabolites (norepinephrine, epinephrine, dopamine) in WT extracts (Fig. 4D).

Total uptake and incorporation of radiolabeled Phe after 2 h into free Phe and Tyr were quantified in the WT, *pah*⁻ and *pah*⁻/+*PAH* lines (Table 1). Total Phe uptake/incorporation was somewhat less in *pah*⁻ (75% WT) and elevated in *pah*⁻/+*PAH* (129% WT), although these differences were not significant. Free Phe was somewhat reduced in *pah*⁻ (78% WT) and more strongly reduced in the *pah*⁻/+*PAH* line (27% WT); again the differences were not significant. As shown in Fig. 4A, *pah*⁻ showed no incorporation of Phe into free Tyr which was strongly significant ($P < 0.01$), while *pah*⁻/+*PAH* showed a 2.4-fold increase.

3.5. PAH and aromatic amino acid growth requirements

To probe the consequences of *PAH* depletion or overexpression, parasites were inoculated into semidefined medium, or this lacking phenylalanine, tryptophan or tyrosine. The WT and *pah*⁻ lines were incapable of sustained proliferation in media lacking any of the aromatic acids (Fig. 5A–C), consistent with the view that *Leishmania* are auxotrophic for aromatic amino acids [43]. Unlike WT cells which arrested at constant cell numbers, *pah*⁻ showed a tendency towards decreased cell numbers over time (Fig. 5A–C).

After a substantial delay of ~8 days, the *pah*⁻/+*PAH* overexpressor was able to resume growth in Tyr-deficient media, although more slowly than in the presence of Tyr (Fig. 5C). These parasites were adapted further by passage in Tyr-deficient media (six passages of 1:100 serial dilutions), and then retested. These P6 *pah*⁻/+*PAH* parasites now exhibited growth in the absence of Tyr comparable to WT in the presence of Tyr (Fig. 5D). Adaptation was dependent on the presence of the episomal *PAH* gene, as WT parasites never increased in their rate of growth (not shown). The basis of adaptation was not studied further but its dependency on episomal *PAH* suggests that increased plasmid copy number and *PAH* expression may account for this finding, as seen originally in 'superselections' of *L. major* episomal vectors [21]. These data provide independent confirmation of the PAH activity of *PAH*, through its role in provision of Tyr under limiting conditions, and alleviation of this requirement when overexpressed.

3.6. Infectivity of *pah*⁻ *L. major* in mouse or macrophage infections

The ability of *pah*⁻ mutant parasites to cause lesions in susceptible BALB/c mice was investigated by inoculating infectious stationary phase promastigotes (10^4 to 10^6) into footpads, and monitoring parasite-induced pathology by measuring footpad thickness over time. For the WT, *pah*⁻ and *pah*⁻/+*PAH* lines, there was no difference in the time until lesion pathology appeared, nor in the progression of lesion pathology thereafter (Fig. 6A and B). Similarly, when inoculated into genetically resistant CBA/J mice, which show transient lesion pathology, all three lines behaved identically (data not shown).

The ability of WT and *pah*⁻ *Leishmania* to survive within peritoneal macrophages was assessed following infection of complement-opsonized stationary phase parasites. Parasitemia was monitored by the percent infected macrophages (Fig. 6C) and

Table 1
Metabolic labeling studies of *L. major* with [^{3}H] Phe.

	Cell line		
	WT	*pah*−	*pah*−/+*PAH*
Total Phe uptake/incorporation	2433 ± 251 (n = 3)	1820 ± 276** (n = 5)	3140 ± 190* (n = 4)
Free phenylalanine	129 ± 49	101 ± 11	34.5 ± 14.4*
Free tyrosine	6.5 ± 1.7	0 (not detectable)***	15.3 ± 10.7

The values shown are pmol [^{3}H]-Phe or Tyr/2.5 × 10^7 cells).
* Statistical significance from WT is indicated as $P < 0.1$.
** Statistical significance from WT is indicated as $P < 0.05$.
*** Statistical significance from WT is indicated as $P < 0.01$.

the number of parasites per 100 macrophages (Fig. 6D). Again, no difference in parasite survival was seen.

3.7. Metacyclogenesis

Previously we showed that H_4B levels were associated with increased differentiation into the infective metacyclic form, which occurs normally following entry into stationary phase [44]. Since PAH activity could affect H_4B levels, we explored the effect of *PAH* depletion or overexpression on metacyclogenesis. Tests were performed in folate-depleted M199 media (fdM199) containing either minimal (0.001 μg ml^{-1}) or saturating (2 μg ml^{-1}) concentrations of biopterin. As before, no differences in growth rate were observed, and metacyclogenesis was elevated under low-biopterin conditions (10–11% vs 4.5–5%; Fig. S2, or data not shown). However, no differences were seen in metacyclogenesis between WT or *pah*− under either condition (Fig. S2). Similar tests showed no effect of epinephrine (100 μM), norepinephrine (100 μM) or propanolol (10 μM) on either parasite growth or differentiation, for either WT or *pah*− (Fig. S2). We conclude that neither *PAH* or the presence of potential downstream effectors arising from PAH activity have any effect on metacyclogenesis, even when grown in the minimum level of biopterin required to support normal growth.

3.8. Reactivity with anti-melanin antibody MAb 6D

Melanin is a downstream metabolite of AAAH activity in many species [45,46] and we used reactivity with the melanin antibody MAb 6D2 to reveal its presence in *Leishmania*. While WT parasites showed no reactivity, comparable to isotypic MAb controls (Fig. 7A or data not shown), when grown in media containing 250 μM DOPA, strong reactivity was observed (Fig. 7C). In contrast, *pah*− parasites showed no reactivity when grown in the presence of DOPA (Fig. 7B). Restoration of PAH expression in the *pah*−/+*PAH* line restored MAb 6D2 reactivity (Fig. 7D). We observed in some but not all experiments that the cells were pigmented in PAH-expressing

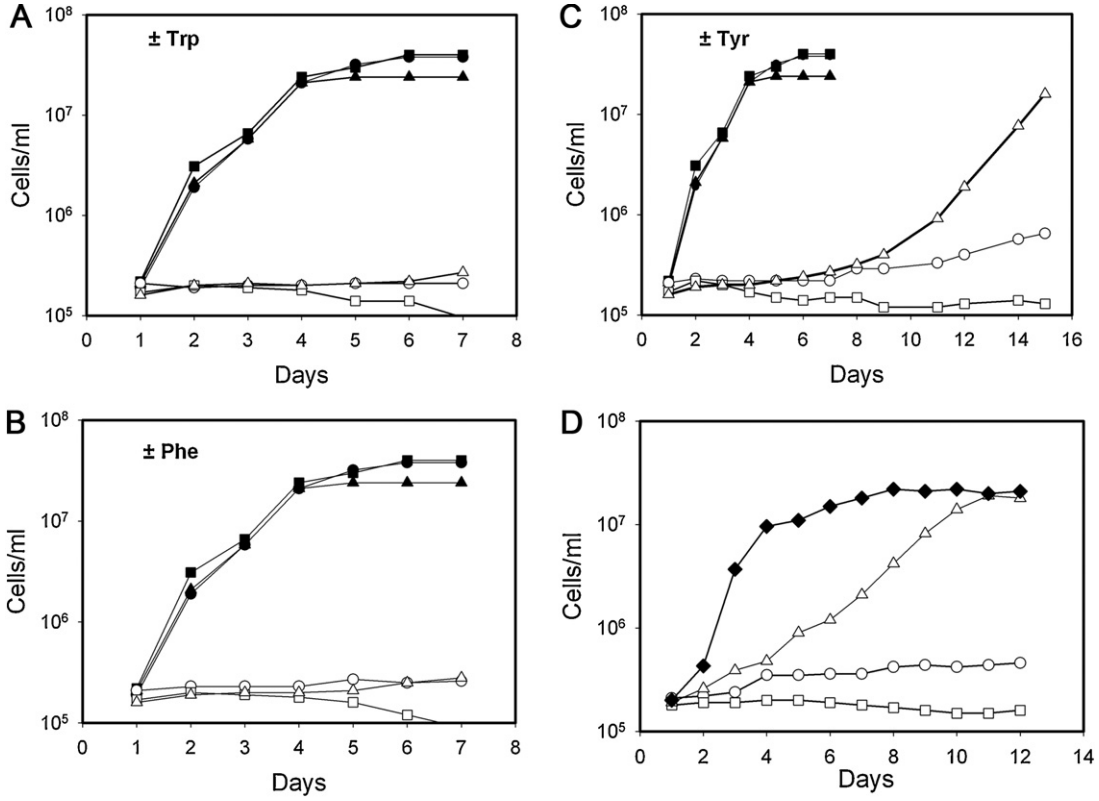

Fig. 5. Growth of *L. major* WT, *pah*− and *pah*−/+*PAH* lines in aromatic amino acid-deficient media. The growth of parasites was measured following inoculation at 2 × 10^5/ml on day 1; all studies were performed at least three times, with a representative experiment shown. Panel A, growth in media containing (dark symbols) or lacking Trp (light symbols). Panel B, growth in media containing (dark symbols) or lacking (open symbols) Phe. Panel C, growth in media containing (dark symbols) or lacking (open symbols) Tyr. Panel D, growth in media lacking Tyr. Cell lines were WT (●, ○), *pah*− (■, □) or *pah*−/+*PAH* (▲, △), or *pah*−/+*PAH* adapted by six serial passages of growth in media lacking Tyr (♦).

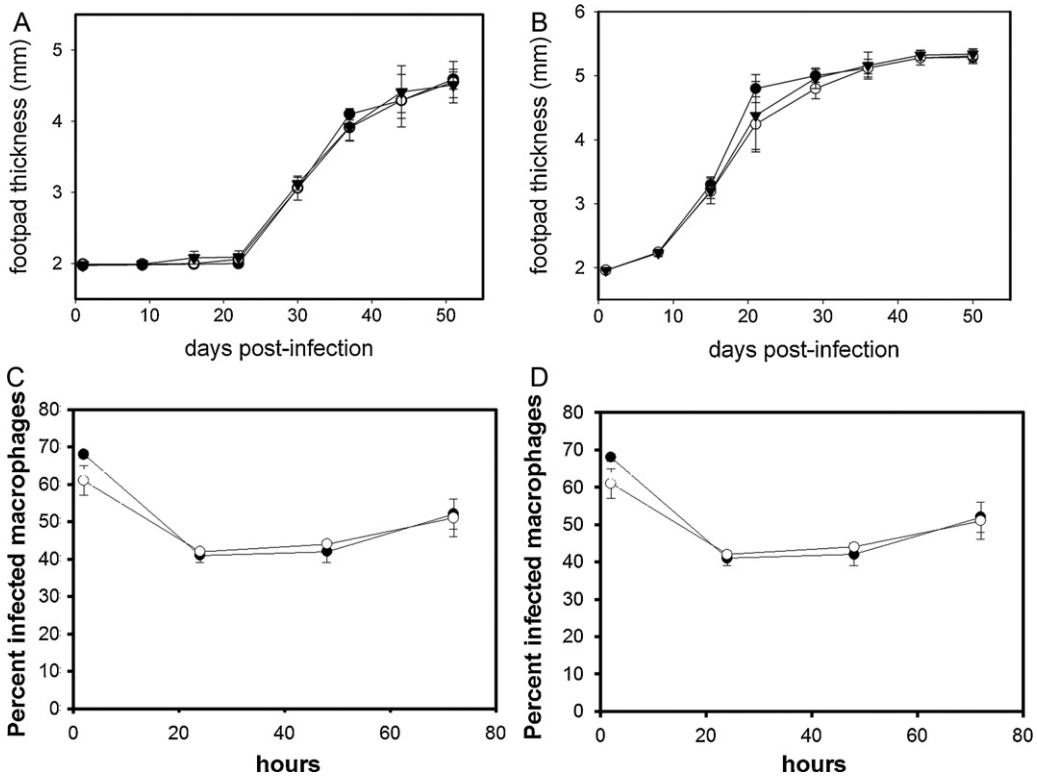

Fig. 6. Virulence of *pah*⁻ promastigotes is not attenuated mouse or macrophage infections. Panels A and B, 10^4 (A) or 10^6 (B) stationary-phase WT or *pah*⁻ parasites were inoculated individually into the footpad of BALB/c mice, and footpad thickness was measured over time. The average and standard deviation from three mice for a representative experiment is shown. Panels C and D, macrophage infections. Survival of complement-opsonized stationary-phase WT or *pah*⁻ is shown. Panels A and B: WT (●), and *pah*⁻ lines KO4 (○) or KO5 (▼). Panel C and D: WT (●) or *pah*⁻ KO4 (○). The average and standard deviation of triplicate determinations from a representative experiment is shown.

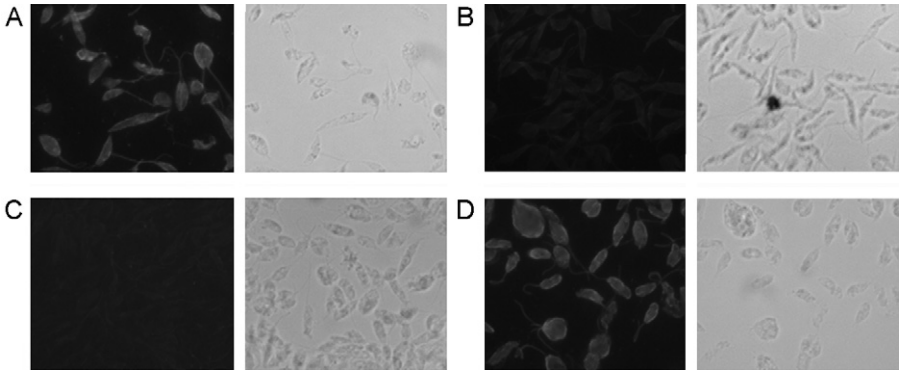

Fig. 7. Immunofluorescence analysis using anti-melanin antibody MAb 6D2. Panel A, WT grown in the presence of L-DOPA; Panel B, *pah*⁻ grown in the presence of L-DOPA; Panel C, WT grown in the absence of L-DOPA; and Panel D, *pah*⁻/+*PAH* grown in the presence of L-DOPA. When added the L-DOPA concentration was 250 μM.

cells grown in the presence DOPA. We sought to confirm that the reactive material was indeed melanin, using a protocol which solubilizes most cellular components but leaves insoluble melanin intact, but were unsuccessful with WT cells grown in the presence of DOPA (not shown).

4. Discussion

In this work we identified and explored potential roles for *L. major* PAH. As we were unable to express active PAH for biochemical characterization, we relied primarily on the predicted properties based on the PAH protein sequence, and the characterization of both a *pah*⁻ null mutant and a *PAH* overexpressor obtained following transfection of a multicopy episomal *PAH* expression vector. Collectively the aromatic amino acid hydroxylase family shares many physical, structural and catalytic properties [4,5,16]. The predicted *L. major* PAH protein showed a typical mammalian-type AAAH domain structure, with a highly conserved central catalytic core flanked by less conserved N terminal and C terminal regions, implicated in regulatory and oligomerization roles in other AAAHs (Fig. 1). The *L. major* PAH central catalytic core showed good conservation of catalytic residues and motifs seen in other AAAHs. Importantly, these residues include those responsible for binding H_4-biopterin.

Several other protozoans bear AAAH genes, including the apicomplexan parasite *Toxoplasma* which has two genes encoding potentially secreted Phe and Trp hydroxylase activity [36], and the cellular slime mold *Dictyostelium* [47]. Phenylalanine hydroxylases also occur sporadically throughout prokaryotes [4,18]. Evolution-

arily, *L. major* PAH falls as expected near the base of the eukaryotic radiation (Fig. S3). While all *Leishmania* species genomes reported to date encode a *PAH* ortholog, it is absent from the genomes of both African and South American trypanosomes. Since a *PAH* gene occurs in the free-living Kinetoplastid relative *Bodo saltans* (family Bodonidae; Fig. S3), we infer that PAH was lost in the common ancestor of trypanosomes following their divergence from *Leishmania*. However, the genome of African trypanosomes predicts a *PCD* gene and trypanosomes express high levels of QDPR activity [13]. This would be consistent with the idea that H_4B is required for essential processes in *Leishmania* and trypanosomes, other than as a cofactor for AAAH activity.

Characterization of the *L. major pah*$^-$ null mutant showed phenotypes firmly establishing the requirement for PAH for phenylalanine hydroxylase activity. While WT parasites converted radiolabeled Phe to Tyr, the *pah*$^-$ mutant was unable to do so (Fig. 4A, Table 1), and correspondingly, the *pah*$^-$/+*PAH* overexpressor showed an elevated ability to do so (Table 1). Despite this activity, WT *L. major* were auxotrophic for Tyr as well as Phe and Trp (Fig. 5A–C), suggesting that WT PAH levels were insufficient for metabolic needs. Notably, WT and PAH overexpressing parasites showed reproducibly higher susceptibility to Phe or Trp deprivation than for Tyr deprivation (Fig. 5C). Moreover, the *pah*$^-$/+*PAH* episomal overexpressor showed only partial growth inhibition, and could be readily adapted for normal growth without Tyr (Fig. 5C and D). These data suggest that WT PAH activity can only partially alleviate Tyr insufficiency, and is able to facilitate cell survival but not full growth. The ability of *PAH* overexpression to rescue Tyr auxotrophy of the *pah*$^-$ mutant firmly establishes the PAH activity of *LmjPAH*.

In contrast to the *PAH*-dependent Phe hydroxylase activity, Tyr or Trp hydroxylase activity was not detected by *in vivo* radiolabeling, using either WT, *pah*$^-$ or the *pah*$^-$/+*PAH* overexpressor. This is consistent with LmjPAH amino acid sequence, which shows residues more typical of AAAHs with Phe rather than Tyr hydroxylase activity (Fig. 1). Correspondingly, PAH expression levels did not alter growth under Phe or Trp deprivation (Fig. 5A and B). These data thus suggest that *Leishmania* PAH is specific for Phe.

4.1. A melanin-like substance in Leishmania?

Curiously, we were able to show reactivity of *Leishmania* against an antibody to melanin, which was dependent on the presence of both PAH and exogenous DOPA (Fig. 7), and in some experiments the *Leishmania* appeared pigmented. However, we failed to recover insoluble acid-resistant pigment characteristic of melanin [30], suggesting that the reactive substance was unlikely to be authentic melanin. A number of melanin-like substances have been described, arising from a variety of diphenolic or other precursors [48]. In the fungus *Cryptococcus neoformans*, melanin plays important roles in virulence [45]. However, since *Leishmania* requires *PAH* to make the melanin-like substance, yet does not require *PAH* for differentiation or infectivity in mice or macrophages (Fig. 7), a role for the melanin-like substance in *Leishmania* virulence seems unlikely.

4.2. PAH null mutants remain viable and virulent

Given the importance of H_4B to *Leishmania* viability and virulence, and that melanin-like substances have been implicated in host-pathogen interactions in several species [36,46,49], we asked whether *PAH*-dependent metabolites played a role in the *Leishmania* infectious cycle. First we examined the ability of the parasite to differentiate to infectious metacyclic parasites *in vitro*, a process known to be up-regulated by low H_4B levels in *L. major* [44]. We confirmed this result, virulent *L. major* FV1 line studied here, but the percent metacyclics was identical between WT and *pah*$^-$ lines when grown in either high or minimal biopterin levels, and nor was it altered in the presence of downstream metabolites including catecholamines or inhibitors (Fig. S2). Similarly, the *pah*$^-$ line behaved identically to WT following infections of primary macrophages *in vitro*, or in infections of susceptible and resistant mice *in vivo* (Fig. 6 or data not shown). Finally, in preliminary studies the *pah*$^-$ line survived well within sand flies, the insect vector of leishmaniasis (D. Sacks, L-FL and SMB, unpublished data).

Thus, while under some circumstances *PAH* can partially mitigate the Tyr growth requirement of *L. major*, it is not essential for normal growth or virulence across the *Leishmania* infective cycle. Similarly, the *PAH* gene is absent in trypanosomes, which like *Leishmania* require H_4B [50]. Future studies may consider other metabolic roles for *PAH*, perhaps in Phe anabolism, drug resistance or in other metabolic pathways such as thioether metabolism [45,51]. However, since the *pah*$^-$ mutant grows normally *in vitro* and *in vivo*, it seems unlikely that PAH activity or PAH-dependent metabolites can account completely for the strong biopterin growth requirement of *Leishmania*.

Acknowledgements

We thank A.H. Fairlamb (U. Dundee) and A. Hanson (U. Florida Gainesville) for discussions, S.C. Daubner and P.F. Fitzpatrick (Texas A&M University) and A. Pribat (U. Florida Gainesville) for assistance and advice in attempts to express active LmjPAH, S. Hickerson for instruction in mouse infectivity tests and macrophage infections, D.L. Sacks (NIH) for preliminary studies of sand fly infectivity, and Tim J. Vickers for comments on this manuscript. This work was supported by National Institutes of Health Grants AI21903 (L-FL, SOK, SMB) and AI52733 (AC, JDN).

Appendix A. Supplementary data

Supplementary data associated with this article can be found, in the online version, at doi:10.1016/j.molbiopara.2010.09.004.

References

[1] Desjeux P. Leishmaniasis: current situation and new perspectives. Comp Immunol Microbiol Infect Dis 2004;27:305–18.
[2] Sacks D, Noben-Trauth N. The immunology of susceptibility and resistance to *Leishmania major* in mice. Nat Immunol 2002;2:845–58.
[3] Opperdoes FR, Coombs GH. Metabolism of *Leishmania*: proven and predicted. Trends Parasitol 2007;23:149–58.
[4] Thony B, Auerbach G, Blau N. Tetrahydrobiopterin biosynthesis, regeneration and functions. Biochem J 2000;347(Pt 1):1–16.
[5] Werner-Felmayer G, Golderer G, Werner ER. Tetrahydrobiopterin biosynthesis, utilization and pharmacological effects. Curr Drug Metab 2002;3:159–73.
[6] Petrillo-Peixoto M, Beverley SM. *In vitro* activity of sulfonamides and sulfones against *Leishmania major* promastigotes. Antimicrob Agents Chemother 1987;31:1575–8.
[7] Beck JT, Ullman B. Nutritional requirements of wild-type and folate transport-deficient *Leishmania donovani* for pterins and folates. Mol Biochem Parasitol 1990;43:221–30.
[8] Kundig C, Haimeur A, Legare D, Papadopoulou B, Ouellette M. Increased transport of pteridines compensates for mutations in the high affinity folate transporter and contributes to methotrexate resistance in the protozoan parasite *Leishmania tarentolae*. EMBO J 1999;18:2342–51.
[9] Cunningham ML, Beverley SM. Pteridine salvage throughout the *Leishmania* infectious cycle: implications for antifolate chemotherapy. Mol Biochem Parasitol 2001;113:199–213.
[10] Bello AR, Nare B, Freedman D, Hardy L, Beverley SM. PTR1: a reductase mediating salvage of oxidized pteridines and methotrexate resistance in the protozoan parasite *Leishmania major*. Proc Natl Acad Sci USA 1994;91:11442–6.
[11] Ouellette M, Drummelsmith J, El-Fadili A, Kundig C, Richard D, Roy G. Pterin transport and metabolism in *Leishmania* and related trypanosomatid parasites. Int J Parasitol 2002;32:385–98.
[12] Nare B, Luba J, Hardy LW, Beverley S. New approaches to *Leishmania* chemotherapy: pteridine reductase 1 (PTR1) as a target and modulator of antifolate sensitivity. Parasitology 1997;114(Suppl.):S101–10.

[13] Lye LF, Cunningham ML, Beverley SM. Characterization of quinonoid-dihydropteridine reductase (QDPR) from the lower eukaryote *Leishmania major*. J Biol Chem 2002;277:38245–53.
[14] Naponelli V, Noiriel A, Ziemak MJ, et al. Phylogenomic and functional analysis of pterin-4a-carbinolamine dehydratase family (COG2154) proteins in plants and microorganisms. Plant Physiol 2008;146:1515–27.
[15] Nare B, Garraway LA, Vickers TJ, Beverley SM. PTR1-dependent synthesis of tetrahydrobiopterin contributes to oxidant susceptibility in the trypanosomatid protozoan parasite *Leishmania major*. Curr Genet 2009;55:287–99.
[16] Fitzpatrick PF. Tetrahydropterin-dependent amino acid hydroxylases. Annu Rev Biochem 1999;68:355–81.
[17] Hufton SE, Jennings IG, Cotton RG. Structure and function of the aromatic amino acid hydroxylases. Biochem J 1995;311(Pt 2):353–66.
[18] Zhao G, Xia T, Song J, Jensen RA. *Pseudomonas aeruginosa* possesses homologues of mammalian phenylalanine hydroxylase and 4 alpha-carbinolamine dehydratase/DCoH as part of a three-component gene cluster. Proc Natl Acad Sci USA 1994;91:1366–70.
[19] Nare B, Hardy LW, Beverley SM. The roles of pteridine reductase 1 and dihydrofolate reductase-thymidylate synthase in pteridine metabolism in the protozoan parasite *Leishmania major*. J Biol Chem 1997;272:13883–91.
[20] da Silva R, Sacks DL. Metacyclogenesis is a major determinant of *Leishmania promastigote* virulence and attenuation. Infect Immun 1987;55:2802–6.
[21] Kapler GM, Coburn CM, Beverley SM. Stable transfection of the human parasite *Leishmania major* delineates a 30-kilobase region sufficient for extrachromosomal replication and expression. Mol Cell Biol 1990;10:1084–94.
[22] Medina-Acosta E, Cross GA. Rapid isolation of DNA from trypanosomatid protozoa using a simple 'mini-prep' procedure. Mol Biochem Parasitol 1993;59:327–9.
[23] Sambrook J, Fritsch EF, Maniatis T. Molecular cloning: a laboratory manual. 1–1000. Cold Spring Harbor Laboratory Press; 1989.
[24] Akopyants NS, Clifton SW, Martin J, et al. A survey of the *Leishmania major* Friedlin strain V1 genome by shotgun sequencing: a resource for DNA microarrays and expression profiling. Mol Biochem Parasitol 2001;113:337–40.
[25] Ryan KA, Dasgupta S, Beverley SM. Shuttle cosmid vectors for the trypanosomatid parasite *Leishmania*. Gene 1993;131:145–50.
[26] Ha DS, Schwarz JK, Turco SJ, Beverley SM. Use of the green fluorescent protein as a marker in transfected *Leishmania*. Mol Biochem Parasitol 1996;77:57–64.
[27] Cruz A, Coburn CM, Beverley SM. Double targeted gene replacement for creating null mutants. Proc Natl Acad Sci USA 1991;88:7170–4.
[28] Goyard S, Beverley SM. Blasticidin resistance: a new independent marker for stable transfection of *Leishmania*. Mol Biochem Parasitol 2000;108:249–52.
[29] Coppi A, Merali S, Eichinger D. The enteric parasite *Entamoeba* uses an autocrine catecholamine system during differentiation into the infectious cyst stage. J Biol Chem 2002;277:8083–90.
[30] Rosas AL, Nosanchuk JD, Feldmesser M, Cox GM, McDade HC, Casadevall A. Synthesis of polymerized melanin by *Cryptococcus neoformans* in infected rodents. Infect Immun 2000;68:2845–53.
[31] Glatman-Freedman A, Martin JM, Riska PF, Bloom BR, Casadevall A. Monoclonal antibodies to surface antigens of *Mycobacterium tuberculosis* and their use in a modified enzyme-linked immunosorbent spot assay for detection of mycobacteria. J Clin Microbiol 1996;34:2795–802.
[32] Titus RG, Muller I, Kimsey P, et al. Exacerbation of experimental murine cutaneous leishmaniasis with CD4+ *Leishmania major*-specific T cell lines or clones which secrete interferon-gamma and mediate parasite-specific delayed-type hypersensitivity. Eur J Immunol 1991;21:559–67.
[33] Titus RG, Marchand M, Boon T, Louis JA. A limiting dilution assay for quantifying *Leishmania major* in tissues of infected mice. Parasite Immunol 1985;7:545–55.
[34] Spath GF, Epstein L, Leader B, et al. Lipophosphoglycan is a virulence factor distinct from related glycoconjugates in the protozoan parasite *Leishmania major*. Proc Natl Acad Sci USA 2000;97:9258–63.
[35] Ivens AC, Peacock CS, Worthey EA, et al. The genome of the kinetoplastid parasite, *Leishmania major*. Science 2005;309:436–42.
[36] Gaskell EA, Smith JE, Pinney JW, Westhead DR, McConkey GA. A unique dual activity amino acid hydroxylase in *Toxoplasma gondii*. PLoS One 2009;4:e4801.
[37] Ramsey AJ, Daubner SC, Ehrlich JI, Fitzpatrick PF. Identification of iron ligands in tyrosine hydroxylase by mutagenesis of conserved histidinyl residues. Protein Sci 1995;4:2082–6.
[38] Erlandsen H, Bjorgo E, Flatmark T, Stevens RC. Crystal structure and site-specific mutagenesis of pterin-bound human phenylalanine hydroxylase. Biochemistry 2000;39:2208–17.
[39] Dickson PW, Jennings IG, Cotton RG. Delineation of the catalytic core of phenylalanine hydroxylase and identification of glutamate 286 as a critical residue for pterin function. J Biol Chem 1994;269:20369–75.
[40] Jiang GC, Yohrling G.Jt., Schmitt JD, Vrana KE. Identification of substrate orienting and phosphorylation sites within tryptophan hydroxylase using homology-based molecular modeling. J Mol Biol 2000;302:1005–17.
[41] Daubner SC, Melendez J, Fitzpatrick PF. Reversing the substrate specificities of phenylalanine and tyrosine hydroxylase: aspartate 425 of tyrosine hydroxylase is essential for L-DOPA formation. Biochemistry 2000;39:9652–61.
[42] Liang XH, Haritan A, Uliel S. Michaeli S. *trans* and *cis* splicing in trypanosomatids: mechanism, factors, and regulation. Eukaryot Cell 2003;2:830–40.
[43] Steiger RF, Steiger E. Cultivation of *Leishmania donovani* and *Leishmania braziliensis* in defined media: nutritional requirements. J Protozool 1977;24:437–41.
[44] Cunningham ML, Titus RG, Turco SJ, Beverley SM. Regulation of differentiation to the infective stage of the protozoan parasite *Leishmania major* by tetrahydrobiopterin. Science 2001;292:285–7.
[45] Nosanchuk JD, Casadevall A. Impact of melanin on microbial virulence and clinical resistance to antimicrobial compounds. Antimicrob Agents Chemother 2006;50:3519–28.
[46] Christensen BM, Li J, Chen CC, Nappi AJ. Melanization immune responses in mosquito vectors. Trends Parasitol 2005;21:192–9.
[47] Siltberg-Liberles J, Steen IH, Svebak RM, Martinez A. The phylogeny of the aromatic amino acid hydroxylases revisited by characterizing phenylalanine hydroxylase from *Dictyostelium discoideum*. Gene 2008;427:86–92.
[48] Plonka PM, Grabacka M. Melanin synthesis in microorganisms—biotechnological and medical aspects. Acta Biochim Pol 2006;53:429–43.
[49] Casadevall A, Rosas AL, Nosanchuk JD. Melanin and virulence in *Cryptococcus neoformans*. Curr Opin Microbiol 2000;3:354–8.
[50] Sienkiewicz N, Ong HB, Fairlamb AH. *Trypanosoma brucei* pteridine reductase 1 is essential for survival in vitro and for virulence in mice. Mol Microbiol 2010.
[51] Steventon GB, Mitchell SC. Phenylalanine 4-monooxygenase and the role of endobiotic metabolism enzymes in xenobiotic biotransformation. Expert Opin Drug Metab Toxicol 2009;5:1213–21.